Molecular Biology of the Cell
Vol. 7, 985–999, June 1996

Multilamellar Endosome-like Compartment Accumulates in the Yeast *vps28* Vacuolar Protein Sorting Mutant

Stephanie E. Rieder,* Lois M. Banta,*† Karl Köhrer,*‡ J. Michael McCaffery, and Scott D. Emr§

Department of Biology, Division of Cellular and Molecular Medicine, Howard Hughes Medical Institute, University of California, San Diego, School of Medicine, La Jolla, California 92093-0668

Submitted January 18, 1996; Accepted March 14, 1996
Monitoring Editor: Randy W. Schekman

In the yeast *Saccharomyces cerevisiae*, vacuolar proteins such as carboxypeptidase Y transit from the Golgi to the lysosome-like vacuole via an endosome-like intermediate compartment. The vacuolar protein sorting (*vps*) mutant *vps28*, a member of the "class E" *vps* mutants, accumulates vacuolar, endocytic, and late Golgi markers in an aberrant endosome-like class E compartment. Sequence analysis of *VPS28* revealed an open reading frame predicted to encode a hydrophilic protein of 242 amino acids. Consistent with this, polyclonal antiserum raised against Vps28p recognized a cytoplasmic protein of 28 kDa. Disruption of *VPS28* resulted in moderate defects in both biosynthetic traffic and endocytic traffic destined for the vacuole. The transport of soluble vacuolar hydrolases to the vacuole was impaired in *vps28* null mutant cells (~40–50% carboxypeptidase Y missorted). Internalization of the endocytic marker FM 4-64, a vital lipophilic dye, resulted in intense staining of a small intracellular compartment adjacent to an enlarged vacuole in Δ*vps28* cells. Furthermore, the vacuolar H^+-ATPase accumulated in the perivacuolar class E compartment in Δ*vps28* cells, as did **a**-factor receptor Ste3p that was internalized from the plasma membrane. Electron microscopic analysis revealed the presence of a novel compartment consisting of stacks of curved membrane cisternae. Immunolocalization studies demonstrated that the vacuolar H^+-ATPase is associated with this cupped cisternal structure, indicating that it corresponds to the class E compartment observed by fluorescence microscopy. Our data indicate that kinetic defects in both anterograde and retrograde transport out of the prevacuolar compartment in *vps28* mutants result in the accumulation of protein and membrane in an exaggerated multilamellar endosomal compartment. We propose that Vps28p, as well as other class E Vps proteins, may facilitate (possibly as coat proteins) the formation of transport intermediates required for efficient transport out of the prevacuolar endosome.

INTRODUCTION

In the yeast *Saccharomyces cerevisiae*, proteins bound for the lysosome-like vacuole traverse the early secretory pathway en route to their final destination (Stevens *et al.*, 1982; reviewed in Stack *et al.*, 1995). Proteins entering this pathway are first translocated from their cytoplasmic site of synthesis into the endoplasmic reticulum (ER), where initial core glycosyl modifications take place, and then transit through the Golgi complex, where the oligosaccharide chains are further modified. In a late Golgi compartment, soluble vacuolar hydrolases such as carboxypeptidase Y (CPY) are actively sorted away from the secretory protein pool (Graham and Emr, 1991) by the vacuolar

* These authors contributed equally to this work.
† Present address: Department of Biology, Haverford College, Haverford, PA 19041.
‡ Present address: Biologisch-Medizinisches Forschungszentrum, Heinrich-Heine Universität, Postfach 10 10 07, 40001 Düsseldorf, Germany.
§ Corresponding author.

protein sorting receptor Vps10p (Marcusson *et al.*, 1994). Vps10p binds to the vacuolar targeting signal of CPY (Marcusson *et al.*, 1994), defined by a short stretch of amino acids within the pro segment of the hydrolase (Johnson *et al.*, 1987; Valls *et al.*, 1987, 1990). Similar to the mannose 6-phosphate receptor in mammalian cells (Kornfeld, 1992), Vps10p appears to deliver CPY to a prevacuolar compartment and recycle back to the late Golgi for further rounds of transport (Cereghino *et al.*, 1995). CPY is then transported to the vacuole, where it is proteolytically cleaved to generate the active mature enzyme.

A number of mutants have been isolated that exhibit defects in the proper localization and processing of multiple vacuolar proteins (Jones, 1977; Bankaitis *et al.*, 1986; Rothman and Stevens, 1986). These *v*acuolar *p*rotein *s*orting (*vps*) mutants constitute more than 45 complementation groups that have been divided into six groups (classes A–F), based on vacuolar morphology and localization of the vacuolar H^+-ATPase (V-ATPase) (Banta *et al.*, 1988; Raymond *et al.*, 1992). The 13 distinct class E *vps* mutants are characterized by a novel structure, the "class E" compartment, that appears to be an exaggerated prevacuolar compartment in which a number of vacuolar, endocytic, and late Golgi markers accumulate (Raymond *et al.*, 1992; Davis *et al.*, 1993; Cereghino *et al.*, 1995; Piper *et al.*, 1995; Vida and Emr, 1995). Several lines of evidence indicate that yeast cells, like mammalian cells, contain an intermediate endosome-like compartment through which vacuolar and endocytosed proteins pass before delivery to the vacuole. For example, yeast cell fractionation studies have demonstrated that there is a post-Golgi, prevacuolar compartment that contains both Golgi-modified CPY and α-factor internalized from the plasma membrane (Singer and Riezman, 1990; Vida *et al.*, 1993). Also, in cells lacking the *YPT7* gene product, a rab7 homologue, endocytosed α-factor accumulates in a nonvacuolar membrane fraction where it is slowly degraded in a proteinase A–dependent manner (Schimmöller and Riezman, 1993).

To gain insight into the mechanism by which vacuolar proteins are transported to the vacuole via the endosome, we characterized the gene and gene product affected in *vps28*, a class E *vps* mutant. Disruption of *VPS28* resulted in the accumulation of vacuolar and endocytic markers in a perivacuolar compartment. This novel compartment consists of stacks of curved membrane cisternae and is proposed to represent an exaggerated prevacuolar endosome, where both biosynthetic and endocytic traffic converge.

MATERIALS AND METHODS

Strains and Media

Bacterial strains were grown on standard media (Miller, 1972). The following *Escherichia coli* strains were used: MC1061 [F^- *araD139 D(araABOIC-leu)7679 ΔlacX74 galU galK rpsL hsdR strA*] (Casadaban and Cohen, 1980), XL1Blue [*supE44 thi-1 lac endA1 gyrA96 hsdR17 relA1 F′ proAB lacI*^{q} *ZΔM15*] (Bullock *et al.*, 1987), and JM101 [*Δ(lac-pro) supE thi-1* F′ *traD36 lacI*^{q} *ZΔM15 proAB*] (Yanisch-Perron *et al.*, 1985).

Saccharomyces cerevisiae yeast strains were grown in standard YPD, SD minimal, Wickerham's minimal proline, and sporulation media (Wickerham, 1946; Sherman *et al.*, 1979). *S. cerevisiae* parental strains were SEY6210 (*MATα ura3–52 leu2–3, 112 his3-Δ 200 trp1-Δ901 lys2–801 suc2-Δ9*), SEY6211 (*MAT*a *ura3–52 leu2–3, 112 his3-Δ200 trp1-Δ901 ade2–101 suc2-Δ9*) (Robinson *et al.*, 1988), and BHY10 [SEY6210 *leu2–3, 112*::pBHY11 (CPY-Inv *LEU2*)] (Horazdovsky *et al.*, 1994). The following yeast strains were also used in this study: SEY28–2 (SEY6210 *vps28–2*) and SEY28–7 (SEY6211 *vps28–7*) (Robinson *et al.*, 1988); SRY28 (SEY6210 *Δvps28::URA3*) and KKY20 (BHY10 *Δvps28::URA3*); TVY1 (SEY6210 *Δpep4::LEU2*) (Vida, unpublished data); and JCY2801 (SEY28–2 *Δpep4::LEU2*) (Cereghino *et al.*, 1995).

Materials

Restriction enzymes, T4 DNA ligase, and Klenow enzyme were purchased from Boehringer Mannheim Biochemicals (Indianapolis, IN). Isopropyl-β-D-thiogalactoside, 5-bromo-4-chloro-3-indolyl-β-D-galactoside, and the Sequenase sequencing kit were obtained from United States Biochemical (Cleveland, OH). 5-fluoroorotic acid was purchased from PCR (Gainesville, FL). Trans^{35}S-label was purchased from ICN Radiochemicals (Irvine, CA). Autofluor was purchased from National Diagnostics (Manville, NJ). Endoglycosidase H was obtained from New England Nuclear (Boston, MA). Zymolyase-100T was purchased from Seikagaku Kogyo (Tokyo, Japan). FM 4-64 [*N*-(3-triethylammoniumpropyl)-4-(*p*-diethylaminophenylhexatrienyl) pyridinum dibromide] and monoclonal antibodies specific for the 60-kDa or 100-kDa vacuolar ATPase subunits were obtained from Molecular Probes (Eugene, OR). The monoclonal antibody specific for the c-myc epitope was purchased from Cambridge Research Biochemicals (Wilmington, DE). The fluorescein isothiocyanate-conjugated goat anti-rabbit immunoglobulin G (IgG) was from Jackson ImmunoResearch (West Grove, PA), while the gold goat anti-mouse IgG conjugate was from Amersham (Deerfield, IL). Antisera against CPY, PrA, and alkaline phosphatase (ALP) have been previously characterized (Robinson *et al.*, 1988; Klionsky *et al.*, 1988, 1989). Antisera recognizing Kex2p and Kar2p were generous gifts of Bill Wickner and Mark Rose, respectively. All other chemicals, including antisera against glucose-6-phosphate dehydrogenase, were purchased from Sigma (St. Louis, MO).

Genetic and DNA Manipulations

Standard recombinant DNA techniques were performed as described (Maniatis *et al.*, 1982; Ausubel *et al.*, 1987). Standard yeast genetic methods were used throughout (Sherman, 1991). Yeast transformations were performed using the lithium acetate method of Ito *et al.* (1983). Genomic yeast DNA was isolated from spheroplasts as described by Sherman *et al.* (1991) and used for Southern blot analysis (Southern, 1975). Radioactive labeled DNA probes were generated according to the method of Feinberg and Vogelstein (1984). Yeast mRNA was isolated by a hot phenol extraction as described previously (Köhrer and Domdey, 1991)

Cloning of VPS28

Yeast strain SEY28–2 carrying plasmid pLJL2 was grown in SD medium lacking leucine to an optical density at 600 nm of 0.5–1.0 and subcultured in YPD for two generations. Plasmid pLJL2 is a derivative of pSEYC306 (Johnson *et al.*, 1987) carrying a *PRC1-SUC2* fusion gene, encoding the amino-terminal 95 amino acids of CPY fused to invertase. Cells were transformed with a yeast genomic library carried on the *E. coli*-yeast shuttle vector YCp50 (*CEN4 ARS1*

URA3) (Rose *et al.*, 1987). Transformants were selected on minimal fructose medium lacking uracil and leucine and screened for external invertase activity using a modification of the rapid filter assay as described previously (Johnson *et al.*, 1987; Klionsky *et al.*, 1988; Paravicini *et al.*, 1992). Transformants exhibiting a wild-type phenotype were cured of the complementing plasmid by incubation on 5-fluoroorotic acid to test for plasmid linkage of the complementing activity.

Plasmid Construction

To determine the minimum complementing region of the original complementing plasmid pLB28–1, various restriction fragments were isolated and subcloned into the appropriate restriction sites within the polylinker of the *E. coli*-yeast shuttle vectors pPHYC16 or pPHYC18 (Herman and Emr, 1990). The resultant plasmids were transformed into the *vps28* mutant strain SEY28–2 carrying pLJL2 and tested for the ability to complement the Vps^- phenotype using the rapid filter assay for external invertase activity.

Plasmid pLB28–104, used for integrative mapping, was constructed by cloning the 4.2-kb *Kpn*I–*Pst*I fragment from pLB28–1 (Figure 1A) into the *Kpn*I/*Pst*I sites of the yeast integrating vector pPHYI10 (*TRP1*, selectable marker) (Herman and Emr, 1990). The resulting plasmid was linearized by cleavage at the unique *Bam*HI site in the cloned DNA to facilitate homologous recombination (Orr-Weaver *et al.*, 1983) and used to transform the *vps28* mutant strain SEY28–2 (*trp1-Δ901*) harboring the plasmid pLJL2. The transformants exhibited no external invertase activity. Two different Trp^+ Suc^- transformants were crossed to the *trp1-Δ901* Suc^- (Vps^+) parental strain SEY6211. Tetrad analysis of the sporulated diploids showed the expected 2 Trp^-:2 Trp^+ segregation pattern; all four spores in each of the nine asci analyzed were Suc^- as assessed by invertase filter assay. An additional 76 random spores were also examined and no Suc^+ segregants were uncovered.

Plasmid pGP28–1 was constructed by subcloning the 3.0-kb *Pvu*II–*Pst*I fragment (Figure 1A) into the *E. coli*-yeast shuttle vector pPHYC16 (Herman and Emr, 1990). A 1.6-kb *Bam*HI fragment containing the entire *VPS28* locus was isolated from pGP28–1 (utilizing the *Bam*HI site in the polylinker) and cloned into the unique *Bam*HI site of the *E. coli*-yeast shuttle vector pRS314 (Sikorski and Hieter, 1989) to yield the centromeric plasmid pKKY281. Plasmid pKKY282 was constructed by cloning the same *Bam*HI fragment into the unique *Bam*HI site of the 2μ vector pJSY324 (Herman *et al.*, 1991).

Plasmid pSP28 was constructed by cloning the 1.5-kb *Bgl*II–*Pst*I fragment shown in Figure 1B into vector pSP72 (Promega, Madison, WI). Construction of plasmid pKKD28, used in the disruption of the *VPS28* gene, was achieved by digesting plasmid pSP28 with *Eco*RI and *Nco*I, blunting the ends with Klenow, and inserting the *URA3* gene from plasmid YEp24 as a blunted 1.2-kb *Hin*dIII fragment (Figure 1B). Plasmid p28-B16, used in the sequencing, contains the 1.6-kb *VPS28* *Bam*HI–*Pst*I fragment (Figure 1A) inserted into the vector pBluescript KS^+ (Stratagene, La Jolla, CA).

Sequence Analysis

The DNA sequence of *VPS28* was obtained by generating exonucleaseIII-mung bean nuclease deletion constructs from the plasmid p28-B16 as described in the Stratagene manual. Double-stranded plasmid DNA templates used for sequencing were isolated by a small scale boiling method (Wilimzig, 1985) and denatured before sequencing. Overlapping clones were sequenced with T3 (5′-ATTAACCCTCACTAAAG-3′)- and T7 (5′-AATACGACTCACTATAG-5′)-specific primers according to the dideoxynucleotide-chain termination method (Sanger *et al.*, 1977) using the Sequenase sequencing kit. Remaining gaps and the second strand were sequenced by using specific oligodeoxynucleotide primers.

Fluorescence Microscopy

Exponentially growing cells were stained with the vital vacuolar dye FM 4-64 as described by Vida and Emr (1995). The method of Redding *et al.* (1991) was used for immunofluorescence with the following modifications: exponentially growing cells were fixed in 4% formaldehyde for 14–18 h, digested with 30 μg/ml Zymolyase 100T to remove the cell wall, and then treated with 1% SDS for 10 min. Fixed spheroplasts were first incubated in monoclonal antibodies specific either for the c-myc epitope or the 60-kDa vacuolar ATPase subunit or 100-kDa vacuolar ATPase subunit, followed by serial incubations of 0.5 μg/ml goat anti-mouse IgG, 1.0 μg/ml rabbit anti-goat IgG, and a 1:100 dilution of fluorescein isothiocyanate-conjugated goat anti-rabbit IgG. Cells used for the immunofluorescent analysis of c-myc–tagged Ste3p were fixed after 6–8 h of growth in 2% galactose-containing medium followed by 60 min of growth in medium with 3% glucose, as described previously (Davis *et al.*, 1993).

Electron Microscopy

Electron microscopy. SEY6210 (*VPS28*) and Δ*vps28* cells were grown in YPD medium at 30°C to an A_{600} of 0.5, harvested by centrifugation, and resuspended in fix (3% glutaraldehyde, 0.1 M sodium cacodylate, 5 mM $CaCl_2$, pH 6.8). Cells were fixed for 1 h at 25°C, washed, and resuspended in 1.2 M sorbitol in phos-citrate buffer (0.1 M K_2HPO_4/0.033 M citric acid). The fixed cells were then treated with glucuronidase and zymolyase for 1 h to remove the cell walls, as described previously (Banta *et al.*, 1988). Cells were embedded in 2% ultra-low gelling temperature agarose (Sigma, type IX), stained with osmium/thiocarbohydrazide as previously described (Banta *et al.*, 1988), and embedded in low viscosity Spurr plastic resin for 48 h at 60°C. Sections were stained with Reynold's lead citrate for 2 min and 2% uranyl acetate for 10 min at 25°C and were viewed at 80 Kv using a JOEL 12 EX transmission electron microscope. The serial sections were cut at a thickness of 100 nm.

Immuno-electron microscopy. Exponentially growing cells at 30°C were fixed in suspension for 15 min by adding an equal volume of fresh fixative (3% paraformaldehyde in phosphate-buffered saline [PBS], pH 7.4) at room temperature. The cells were pelleted and resuspended in fresh fixative for an additional 12–15 h. The cells were then washed briefly in PBS and resuspended in 1% low gelling temperature agarose. The agarose blocks were trimmed into mm^3 pieces, cryoprotected by infiltration with a mixture of 2.3 M sucrose/20% polyvinyl pyrrolidone (10K)/PBS (pH 7.4) for 2 h, and then mounted on cryo-pins and rapidly frozen in liquid nitrogen. Ultrathin cryosections were cut on a Reichert Ultracut-E ultramicrotome equipped with an FC-4 cryoattachment and collected onto formvar/carbon-coated nickel grids. The grids were washed through several drops of 5% fetal calf serum-PBS containing 0.01 M glycine (pH 7.4), blocked in 10% fetal calf serum-PBS, and incubated overnight with 10 μg/ml monoclonal antibody specific to the 60-kDa vacuolar ATPase subunit. After washing, the grids were incubated for 2 h with a 10-nm gold goat anti-mouse IgG conjugate. The grids were washed several times in PBS followed by several drops of ddH_2O and subsequently embedded in an aqueous solution containing 2.7% polyvinyl alcohol (10K)/0.2% methyl cellulose (400 centipoises)/0.2% uranyl acetate. The sections were observed and photographed on a Philips CM 10 or JEOL 1200EX II transmission electron microscope.

Vps28p-specific Antibody Production

A *trpE-VPS28* gene fusion was constructed by cloning a 750-bp *Eco*RI–*Hin*dIII fragment, encoding the carboxy-terminal 160 amino acids of Vps28p (Figure 1A), into the *Eco*RI/*Hin*dIII sites of the vector pATH3 (Dieckmann and Tzagoloff, 1985). The TrpE-Vps28 fusion protein was expressed in *E. coli* XL1Blue cells, purified, and used to inoculate white male New Zealand rabbits (Paravicini *et al.*, 1992).

Cell Labeling, Immunoprecipitation, and Subcellular Fractionation

To analyze the sorting and transport of vacuolar proteins, yeast cells were grown at 30°C in minimal medium supplemented with amino acids to an optical density at 600 nm (OD_{600}) of 0.5–1.0. Cells were harvested by centrifugation and converted into spheroplasts as described previously (Paravicini *et al.*, 1992). The spheroplasts were resuspended in 0.5 ml of YNB containing 1 mg/ml of bovine serum albumin and 100 μg/ml of α_2-macroglobulin. Cells were preincubated at 30°C for 5 min and then labeled for 10 min at 30°C with 100 μCi of Trans^{35}S-label. Chase was initiated by the addition of methionine, cysteine, and yeast extract to final concentrations of 5 mM, 1 mM, and 0.2%, respectively. Following a 0- or 45-min chase period, the cultures were centrifuged at 13,000 × *g* for 1 min to generate an intracellular (pellet) fraction and an extracellular (supernatant) fraction. The presence of CPY, PrA, and ALP proteins in each fraction was determined by immunoprecipitation, SDS-PAGE, and fluorography (Klionsky *et al.*, 1988; Robinson *et al.*, 1988). Radioactive immunoprecipitates were treated with endoglycosidase H as in Graham *et al.* (1994).

For immunodetection of Vps28p, whole yeast cells were labeled with Trans^{35}S-label as described previously (Paravicini *et al.*, 1992), except that the chase was initiated by addition of one volume of Wickerham's minimal proline medium containing 10 mM methionine and 0.4% yeast extract.

Subcellular fractionation was performed as described previously (Köhrer and Emr, 1993).

RESULTS

Cloning and Genetic Analysis of VPS28

vps28 mutants were isolated by selecting for mutations in *S. cerevisiae* that result in the missorting and secretion of a hybrid protein that consisted of the vacuole targeting signal of CPY fused to the invertase protein (Inv). Invertase is a secreted enzyme required for conversion of sucrose into glucose and fructose. In Vps$^+$ cells deleted for endogenous invertase genes, the hybrid protein CPY-Inv is diverted to the vacuole and no external invertase activity is generated; thus these cells are unable to grow on sucrose as the sole carbon source (Suc$^-$ phenotype) (Johnson *et al.*, 1987). However, in mutant cells that missort the CPY-Inv fusion protein, invertase activity is detected at the cell surface and thus these cells are able to utilize sucrose (Suc$^+$) (Bankaitis *et al.*, 1986; Robinson *et al.*, 1988). *vps28* mutants secrete ~30–40% of the CPY-Inv hybrid protein and are also defective in the localization of CPY as well as two other soluble vacuolar hydrolases, proteinase A (PrA) and proteinase B (Robinson *et al.*, 1988).

We have previously described a simple colorimetric plate assay for secreted invertase activity that enabled us to screen for complementation of the vacuolar protein sorting defect (Vps$^-$) of *vps28* mutant cells (Paravicini *et al.*, 1992). We transformed SEY28–2 with a yeast genomic library to generate 12,000 transformants, one of which was found to be reproducibly Suc$^-$ (Vps$^+$). This transformant was Suc$^+$ when cured of the *URA3* library plasmid, indicating that the Suc$^-$ phenotype was plasmid-linked. The recovered complementing plasmid restored vacuolar localization of the CPY-Inv hybrid protein in both SEY28–2 as well as a strain carrying a different allele of *vps28* (SEY28–7).

A partial restriction map of the insert in the complementing plasmid, designated pLB28–1, is shown in Figure 1A. Subcloning of the original 11-kb insert and complementation analysis revealed that the complementing activity resided on the 3-kb *Pvu*II–*Pst*I fragment indicated in Figure 1A. Integrative mapping experiments, described in MATERIALS AND METHODS, confirmed that the complementing clone was tightly linked to the *VPS28* locus.

VPS28 Sequence Analysis

The nucleotide sequence of *VPS28* was determined by sequencing both strands of the 1.6-kb *Bam*HI–*Pst*I fragment (Figure 1A) as described in MATERIALS AND METHODS. The sequence revealed a single open reading frame predicted to encode a 242-amino acid protein of 27,700 Da (Figure 2A). A consensus sequence for transcription initiation (TATAAA) (Struhl, 1987) was identified 200 bp upstream of the putative translational start site. A sequence (TAG... TATG... TTT) that closely resembles a proposed transcription termination consensus sequence (Zaret and Sherman, 1982) was found starting 13 bp downstream of the stop codon. In accordance with these observations, a single RNA species of approximately 1-kb was detected by Northern analysis (Figure 1C). The predicted amino acid sequence for the Vps28 protein

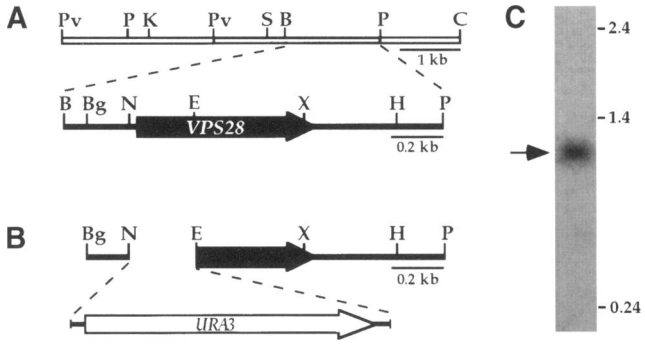

Figure 1. Characterization and disruption of the *VPS28* locus. (A) Restriction map of a portion of the 11-kb insert in the complementing plasmid pLB28–1. Restriction site abbreviations are as follows: B, *Bam*HI; Bg, *Bgl*II; C, *Cla*I; K, *Kpn*I; P, *Pst*I; Pv, *Pvu*II; and S, *Ssp*I. The minimum complementing region is indicated by the gray section; the location, size, and orientation of the *VPS28* open reading frame is indicated by the black arrow below. (B) Disruption of the *VPS28* gene. Plasmid pKKD28, in which the *URA3* gene replaced the 310-bp *Nco*I–*Eco*RI fragment of the *VPS28* gene, was used to generate the Δ*vps28* mutants (SRY28 and KKY20). Additional restriction site abbreviations are as follows: H, *Hin*dIII; R, *Eco*RI; N, *Nco*I; and X, *Xba*I. (C) *VPS28* transcript. The mRNA corresponding to *VPS28* was identified by Northern analysis using the 990-nt *Ssp*I-*Hin*dIII fragment as a probe.

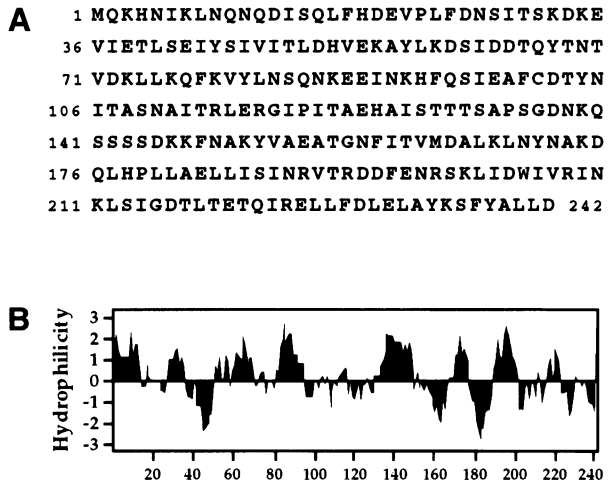

Figure 2. The deduced amino acid sequence and hydropathy analysis of Vps28p. (A) The *VPS28* gene is predicted to encode a 242-amino acid protein. (B) Hydropathy analysis of the deduced Vps28p amino acid sequence according to the algorithm of Kyte and Doolittle (1982). Hydrophilic regions are shown above the axis; hydrophobic regions are below the axis.

(Vps28p) is generally hydrophilic and does not appear to contain an amino-terminal signal sequence or any hydrophobic regions of sufficient length to span a lipid bilayer (Figure 2B). Comparison of the amino acid sequence to the GenEMBL and Swiss Prot databases revealed no significant homologies to other known proteins or sequence motifs.

Disruption of VPS28 Resulted in a Moderate Vacuolar Protein Sorting Defect

A *vps28* null mutant strain was generated by disrupting the *VPS28* locus using the one-step gene disruption technique (Rothstein, 1983). The 310-nucleotide *Nco*I–*Eco*RI fragment shown in Figure 1B was replaced with the *URA3* gene in plasmid pSP28 to generate plasmid pKKD28. This plasmid was digested with *Bgl*II and *Sph*I (utilizing a *Sph*I site in the polylinker) and used to transform the haploid strains SEY6210 (SRY28) and BHY10 (KKY20). Ura^+ transformants were picked, and the disruption of the *VPS28* gene was confirmed by Southern blotting experiments.

To assess the effect of deleting *VPS28* on vacuolar protein sorting, the fate of newly synthesized CPY was examined. Spheroplasts were metabolically labeled for 10 min with Trans^{35}S-label and chased for 0 or 45 min by the addition of unlabeled cysteine and methionine. The cultures were separated into spheroplast (intracellular, I) and media (extracellular, E) fractions by centrifugation. The distribution and size of CPY was then determined by immunoprecipitation, SDS-PAGE, and fluorography. In wild-type cells, the ER-modified (p1CPY; 67 kDa) and the Golgi-modified (p2CPY; 69 kDa) precursor forms of CPY present after a 10-min pulse were completely converted to intracellular mature CPY (mCPY; 61 kDa) within the 45-min chase period (Figure 3A, lanes 1–4). In contrast, Δ*vps28* (SRY28) cells secreted approximately 40–50% of the newly synthesized CPY as the Golgi-modified p2CPY precursor form (Figure 3A, lanes 5–8). Essentially all of the missorted p2CPY was found in the extracellular fraction after a 10-min chase, indicating that the secretory pathway is intact and can rapidly deliver the missorted p2CPY to the cell surface in Δ*vps28* cells. Most of the remaining CPY (50–60%) was processed to the mature form in Δ*vps28* cells, indicating that it had been transported to a compartment containing active vacuolar hydrolases (Figure 3A, lanes 5–8). The processing kinetics of the properly matured CPY in Δ*vps28* cells was similar to that observed in wild-type cells. The sorting defect exhibited by Δ*vps28* cells was corrected by the wild-type *VPS28* gene carried on either a centromeric (lanes 9–10) or a 2μ-overexpressing plasmid. The amount of missorted CPY observed

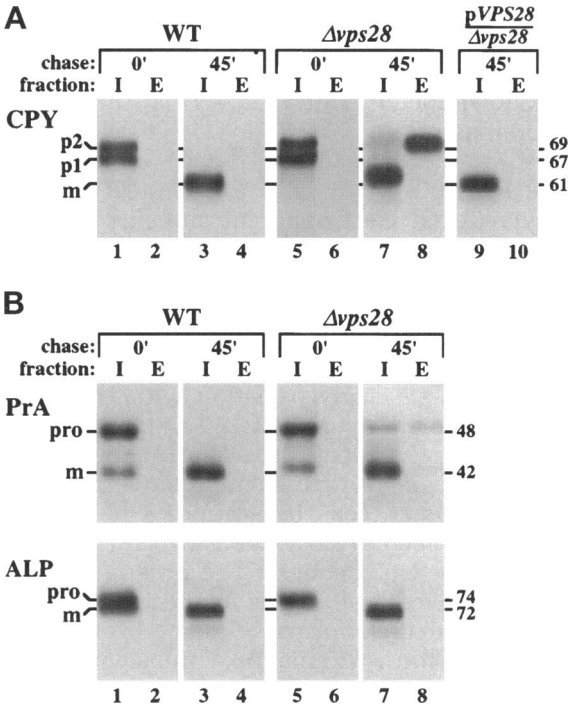

Figure 3. Intracellular sorting of vacuolar hydrolases in Δ*vps28* mutant cells. Yeast spheroplasts were labeled with Trans^{35}S-label for 10 min, chased for 0 or 45 min, and separated into intracellular (I) and extracellular (E) fractions. The presence of (A) CPY and (B) PrA and ALP in these fractions was determined by immunoprecipitation. The molecular masses of the precursor and mature forms of these vacuolar enzymes are indicated in kilodaltons. The migration positions of precursor and mature vacuolar hydrolases in wild-type cells are indicated by horizontal lines. The following strains were used: lanes 1–4, SEY6210 (wild type); lanes 5–8, SRY28 (Δ*vps28*); and lanes 9–10, SRY28 carrying the *CEN*-based plasmid pKK281.

in Δ*vps28* cells is similar to that observed in cells harboring original alleles of *vps28*, suggesting that these cells produce little or no active Vps28p.

The sorting and processing of two other vacuolar hydrolases, PrA and ALP, were also examined in the Δ*vps28* cells. In wild-type cells, the soluble vacuolar protein PrA was found as its 48-kDa precursor form (proPrA) after a 10-min pulse and was completely processed to the 42-kDa mature vacuolar form by 45 min of chase (Figure 3B, lanes 1–4). In the Δ*vps28* mutant strain, 10–15% of PrA remained in the proPrA form after the 45-min chase (Figure 3B, lanes 7–8). However, the missorted proPrA was not secreted to the same extent as p2CPY (Figure 3B, lane 8).

In contrast to what we observed with CPY and PrA sorting in Δ*vps28* cells, the vacuolar integral membrane protein ALP was entirely processed to the 72-kDa mature form (mALP) in Δ*vps28* cells during the 45-min chase (Figure 3B, lanes 5–8). However, the transport and/or processing of ALP is slightly delayed in Δ*vps28* cells (Figure 3B, lanes 1 and 5), as indicated by the slightly lower abundance of mALP in Δ*vps28* cells compared with wild-type cells after the 10-min pulse. Indirect immunofluorescence (Raymond *et al.*, 1992) and subcellular fractionation studies (Cereghino *et al.*, 1995) indicate that ALP localizes to the vacuolar membrane of class E *vps* mutant cells; therefore, maturation of ALP in Δ*vps28* cells is consistent with proper localization of ALP to the vacuole.

In Δ*vps28* cells, both p2CPY and mCPY exhibited slightly reduced electrophoretic mobility relative to that observed in wild-type cells (Figure 3A). In contrast, p1CPY from Δ*vps28* cells and wild-type cells exhibited identical mobility under these conditions. This phenotype was also observed in a subset of other class E *vps* mutants (i.e., *vps22*, *vps23*, *vps25*, *vps32*, and *vps36*). Following deglycosylation with endoglycosidase H, the mobility of p2CPY and mCPY in the Δ*vps28* strain was identical to that in the wild-type strain. The observed increase in the molecular weight of CPY in Δ*vps28* cells thus appears to be due to increased N-linked glycosylation, which probably occurs within the Golgi complex, because of the following: 1) the ER form of CPY is unaffected, 2) both the secreted and mature forms of CPY are overglycosylated, and 3) the α1,3-mannosyltransferase Mnn1p (Graham *et al.*, 1994) appears to maintain its normal Golgi distribution in class E *vps* mutants (Cereghino *et al.*, 1995). Both precursor and mature forms of PrA and ALP were also slightly overglycosylated in Δ*vps28* cells (Figure 3B, lanes 1–8); however, the molecular weight change is less noticeable for these proteins than for CPY, probably because they have fewer oligosaccharide side chains than CPY. A slight delay in movement of vacuolar proteins through the Golgi complex may increase the length of time a protein such as CPY is exposed to the glycosyltransferases.

The phenotypic similarities among the 13 different class E *vps* mutants suggest that the class E Vps proteins may function at a common step in the vacuolar protein sorting pathway. To test this hypothesis, over 20 class E *vps* double mutants were constructed (i.e., *vps28/vps27*, *vps28/vps2*, *vps28/vps4*, *vps25/vps27*, *vps20/vps27*, and *vps27/vps22*). Each of the double class E *vps* mutants exhibited vacuolar protein sorting phenotypes similar to the single class E *vps* mutant strains.

The secretory pathway is not significantly impaired by the loss of Vps28p, as indicated by the rapid secretion of the missorted p2CPY from Δ*vps28* cells (Figure 3A, lanes 7 and 8). To further analyze protein secretion in *vps28* mutant cells, the transport of multiple secreted proteins was examined in Δ*vps28* and wild-type cells. Cells were pulsed with Trans^{35}S-label at 30°C for 20 min. After a 10- or 40-min chase period, cells were removed by centrifugation, and secreted proteins in the media were precipitated with 10% trichloroacetic acid and analyzed by SDS-PAGE. The set of detected proteins and their rate of secretion in Δ*vps28* cells was similar to that of wild-type cells. Taken together, these results suggest that the transport pathway between the ER and the plasma membrane is not significantly perturbed in *vps28* mutant cells.

Identification and Characterization of the VPS28 Gene Product

A TrpE-Vps28 fusion protein was used to generate Vps28p-specific antiserum. The fusion protein, which included the carboxyl-terminal 160 amino acids of Vps28p, was expressed in *E. coli* cells, purified, and used to immunize rabbits. The resulting antiserum immunoprecipitated a single protein of 28 kDa from wild-type yeast extracts that were radiolabeled for 10 min with Trans^{35}S-label and chased for 15 or 60 min (Figure 4A, lanes 2 and 3). This polypeptide was not recognized by the preimmune serum and was not seen in Δ*vps28* cells (Figure 4A, lane 1). The abundance of Vps28p did not diminish over a 60-min chase, indicating that the protein is relatively stable (Figure 4A, lanes 2 and 3). In yeast cells carrying the *VPS28* gene on a 2μ-overexpressing plasmid, the polypeptide recognized by the antiserum was ~40–50 fold more abundant (Figure 4A, lane 4). This high level of Vps28p overexpression did not affect cell growth or vacuolar protein sorting.

Although the predicted Vps28p sequence contains two potential sites for N-linked glycosylation (residues 105 and 198), endoglycosidase H treatment of Vps28p immunoprecipitated from radiolabeled wild-type cell extracts did not affect the protein's mobility on SDS-polyacrylamide gels, indicating that neither site is utilized. This observation is consistent with the absence of a putative signal sequence that would mediate entry into the secretory pathway.

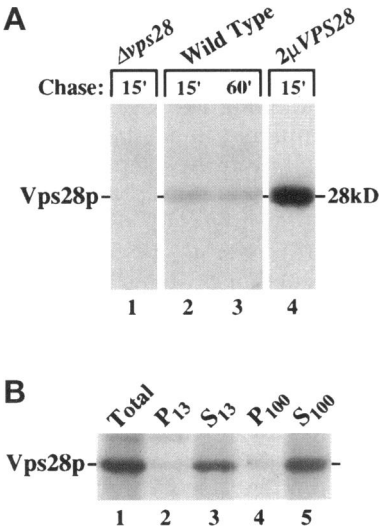

Figure 4. Immunoprecipitation and subcellular fractionation of Vps28p. (A) Cells were labeled for 10 min, chased for either 15 or 60 min, and subjected to immunoprecipitation with antiserum raised against a TrpE-Vps28 fusion protein. Strains used were as follows: BHY10 (wild type), KKY20 (Δ*vps28*), and BHY10 carrying plasmid pKK282 (2μ*VPS28*). (B) Wild-type spheroplasts (BHY10) were labeled for 15 min and chased for 45 min before lysis in triethanolamine buffer. After centrifugation at 500 × *g* to remove unlysed spheroplasts, the supernatant ("total") was spun at 13,000 × *g* to generate supernatant (S_{13}) and pellet (P_{13}) fractions. A portion of the S_{13} was centrifuged again at 100,000 × *g* to generate supernatant (S_{100}) and pellet (P_{100}) fractions. The presence of Vps28p in each fraction was determined by quantitative immunoprecipitation. The distribution of marker proteins for the vacuole (ALP), the late Golgi compartment (Kex2p), and the cytosol (glucose-6-phosphate dehydrogenase) in each fraction was determined by immunoprecipitation and is summarized in Table 2.

Subcellular fractionation was used to assess the intracellular location of Vps28p. Spheroplasts of the wild-type strain BHY10 were labeled with Trans^{35}S-label for 15 min, chased for 45 min, and then lysed by homogenization in triethanolamine lysis buffer (Köhrer and Emr, 1993). The cleared cell lysate (500 × *g* supernatant fraction, "Total") was subjected to centrifugation at 13,000 × *g* to generate pellet (P_{13}) and supernatant (S_{13}) fractions. A portion of the S_{13} was then spun at 100,000 × *g* to generate a high-speed pellet and supernatant (P_{100} and S_{100}). The resulting fractions were subjected to immunoprecipitation, using antisera that recognize either Vps28p or various marker proteins. We found that >90% of Vps28p was in the nonsedimentable fraction (S_{100}; Figure 4B, lane 5). This distribution of Vps28p was similar to that of the cytosolic marker enzyme glucose-6-phosphate dehydrogenase, which is found exclusively in the S_{100} fraction (Table 1). In contrast, the vacuolar marker mALP was primarily found in the P_{13} fraction (>90%), while the majority (>90%) of the late Golgi marker Kex2p was found in the P_{100} fraction (Table 1). Similar results were obtained using a 50 mM Tris/0.2 M sorbitol/0.5 mM EDTA lysis buffer. Thus Vps28p behaves like a soluble cytosolic protein under the conditions used for these fractionations.

Table 1. Subcellular distribution of Vps28p and marker proteins

Protein	P_{13}	P_{100}	S_{100}
Vps28p	<5%	<5%	>90%
Alkaline phosphatase (vacuole membrane)	90%	10%	
Kex2p (Golgi membrane)	10%	90%	
Glucose-6-P dehydrogenase (cytosol)			100%

Δvps28 Cells Accumulate Biosynthetic and Endocytic Markers in an Exaggerated Endosome-like Compartment

To examine the impact of the loss of Vps28p on the endocytic pathway and vacuolar morphology, Δ*vps28* cells were stained with the lipophilic styryl dye FM 4-64. This vital fluorescent dye initially stains the plasma membrane and then is internalized and delivered to the vacuolar membrane in a time-, energy-, and temperature-dependent manner (Vida and Emr, 1995). Thus FM 4-64 appears to serve as a marker for bulk membrane endocytosis in yeast (Vida and Emr, 1995). In wild-type cells stained with FM 4-64, the vacuole appeared as one to three irregularly shaped fluorescent compartments (Figure 5A). In Δ*vps28* cells, however, an enlarged spherical vacuole was observed; furthermore, we observed pronounced staining of a small compartment adjacent to the vacuole (Figure 5B). One or sometimes two of these small perivacuolar structures, which presumably correspond to the class E compartment, were found in essentially all Δ*vps28* cells examined (>90%). Δ*vps28* cells carrying the wild-type *VPS28* gene on a CEN-plasmid (pKKY281) exhibited a vacuolar morphology that was indistinguishable from that of the wild-type strain. These results suggest that, in addition to defects in vacuolar protein sorting, *vps28* cells may also have a defect in endocytosis.

We extended our analysis of endocytosis in Δ*vps28* cells by monitoring the distribution of the plasma membrane **a**-factor receptor Ste3p, which is internalized and delivered to the vacuole for degradation in wild-type cells (Davis *et al.*, 1993). For these experiments, we utilized a c-myc epitope-tagged Ste3p expressed under the control of the galactose-inducible promoter *GAL* (Davis *et al.*, 1993) and the protease-deficient strains TVY1 (*VPS28* Δ*pep4*) and JCY2801 (*vps28–2* Δ*pep4*) to stabilize Ste3p. Cells were grown in 2% galactose for 6–8 h to induce Ste3p production, followed by a 60-min chase in media containing 3% glucose. The cells were then fixed and prepared for

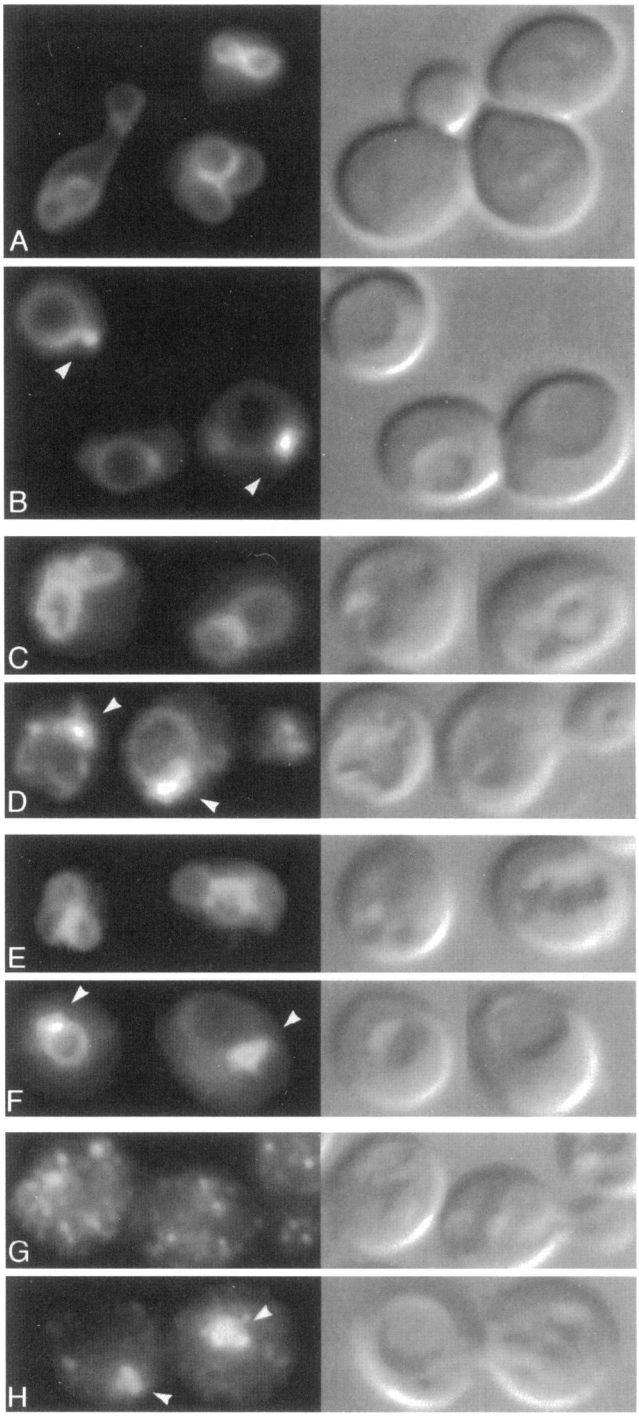

Figure 5. *vps28* mutant cells accumulate endocytic and biosynthetic markers in a perivacuolar endosome-like compartment. (A) Wild-type (SEY6210) and (B) Δ*vps28* (KKY20) cells were treated with the vital endocytic marker FM 4-64 for 15 min followed by a 45-min chase period. The stained cells were visualized by fluorescence (left panels) and Nomarski (right panels) microscopy. The distribution of endocytosed c-myc epitope-tagged Ste3p in (C) *VPS28* Δ*pep4* (TVY1) and (D) *vps28–2* Δ*pep4* (JC2801) was visualized by indirect immunofluorescence with monoclonal antibodies specific for the c-myc epitope. The distribution of the vacuolar H^+-ATPase in (E) wild-type (SEY6210) and (F) Δ*vps28* (KKY20) cells was examined by indirect immunofluorescence using monoclonal antibodies specific for the 60-kDa subunit of the V-ATPase. The distribution of endocytosed c-myc epitope-tagged Vps10p in (G) *VPS28* Δ*pep4* (TVY1) and (H) *vps28–2* Δ*pep4* (JC2801) was visualized by indirect immunofluorescence with monoclonal antibodies specific for the c-myc epitope. The white arrowheads indicate examples of the exaggerated prevacuolar compartments seen in *vps28* mutant cells.

indirect immunofluorescence with a monoclonal antibody specific to the c-myc epitope. In wild-type cells, Ste3p was efficiently delivered from the plasma membrane to the vacuole (Figure 5C). In Δ*vps28* cells, however, Ste3p accumulated in a small compartment near the vacuole as well as in the vacuolar membrane (Figure 5D). These results are in accordance with analyses of Ste3p distribution in class E *ren1/vps2* (Davis *et al.*, 1993) and *vps27* (Piper *et al.*, 1995) mutant cells.

To determine whether proteins transported from the late Golgi to the vacuole also accumulate in the perivacuolar class E compartment, indirect immunofluorescence of the V-ATPase was performed. The V-ATPase, a multi-subunit enzyme that consists of both peripheral membrane proteins (V_1 complex) and integral membrane proteins (V_0 complex), establishes the acidic environment needed for efficient activation of vacuolar hydrolases (Jones, 1984; Anraku *et al.*, 1992; Kane and Stevens, 1992; Nelson, 1992). In wild-type cells, the 60-kDa V-ATPase (V_1 complex) subunit was associated with vacuolar membranes, indicating that the V-ATPase was properly assembled on the vacuolar membrane (Figure 5E). In Δ*vps28* cells, the V-ATPase was found in both the class E compartment and in the vacuole (Figure 5F). Also, a modest cytoplasmic staining is observed in Δ*vps28* cells (Figure 5F), suggestive of unassembled V-ATPase subunits. To further investigate this, indirect immunofluorescence was performed using antibody specific to an epitope of the integral membrane 100-kDa subunit that is masked when the V-ATPase is properly assembled (Kane *et al.*, 1992). No staining was observed in wild-type cells; however, in Δ*vps28* cells, the class E compartment was stained. Although some of the V-ATPase that accumulates in the class E compartment is not properly assembled, the majority of the V-ATPase found in the class E compartment appears to be assembled and functioning; quinacrine staining in *vps28* cells indicates that the class E compartment is acidified, and a substantial portion of the 60-kDa V-ATPase subunit localized to this compartment.

Previous results suggest that recycling from the endosome back to the late Golgi is impaired in *vps28* and the other class E *vps* mutants (Cereghino *et al.*, 1995). In these mutants, the vacuolar protein sorting receptor Vps10p (Marcusson *et al.*, 1994) is rapidly cleaved in a *PEP4*-dependent manner in a nonvacuolar compart-

ment that appears to be the class E compartment (Cereghino *et al.*, 1995). To further investigate the subcellular localization of Vps10p in *vps28* mutant cells, indirect immunofluorescence was performed in TVY1 (*VPS28* Δ*pep4*) and JCY2801 (*vps28–2* Δ*pep4*) strains that expressed a c-myc epitope-tagged version of Vps10p encoded by pEMY10–21 (Cereghino *et al.*, 1995). Indirect immunofluorescence with monoclonal antibody against the c-myc epitope revealed a punctate staining pattern TVY1 cells, consistent with localization of Vps10p to the Golgi and endosomes (Figure 5G). In JCY2801 cells, however, the c-myc epitope-tagged Vps10p primarily accumulated in the class E compartment (Figure 5H). A similar distribution of Vps10p has also been observed in class E *vps27* mutant cells (Piper *et al.*, 1995). The accumulation of Vps10p in the class E compartment in *vps28* mutant cells is consistent with a defect in recycling from the endosome back to the late Golgi in class E *vps* mutants.

Δ*vps28* Cells Accumulate Stacks of Curved Cisternal Membranes

To investigate the morphological changes caused by the loss of Vps28p, we examined Δ*vps28* cells by electron microscopy. This analysis revealed the striking presence of novel multilamellar membrane structures in Δ*vps28* cells that consisted primarily of stacks of curved membrane cisternae (Figure 6B). Figure 6, C–D, depicts enlarged images of the cupped cisternae found in Δ*vps28* cells. Twenty percent of the Δ*vps28* cell sections examined (n = 145) contained multilamellar structures similar to those shown in Figure 6, B–D, while none of the 151 wild-type cell sections contained such structures (Figure 6A). In addition, smaller stacks of cupped membranes as well as fenestrated and tubular membrane compartments were observed more frequently in Δ*vps28* sections than in wild-type sections. Some of the curved membrane cisternae were flattened with little lumenal space, while others were dilated with apparent content. Given that nuclei were seen in ~65% of the Δ*vps28* sections and that the cisternal structures (Figure 6, B–D) often had a diameter of about one-third that of the nucleus, the observed frequency of the cupped stacks of cisternae (20%) is consistent with almost all Δ*vps28* cells containing such stacks of curved cisternae.

To gain further insight into the organization of this unique structure, 100-nm serial sections of Δ*vps28* cells were examined by electron microscopy. The novel multilamellar compartment generally consisted of either loosely cupped stacks of membrane cisternae (Figure 7, A–F) or of more spherical structures of curved cisternae (Figure 7, G–J). Fenestrated and tubular membrane structures were also observed (Figure 7, C–E). None of the curved cisternae appeared to form closed continuous membrane rings in the observed sections (Figure 7). Sections through numerous cells indicated that these exaggerated organelles are found at a frequency of about one per Δ*vps28* cell.

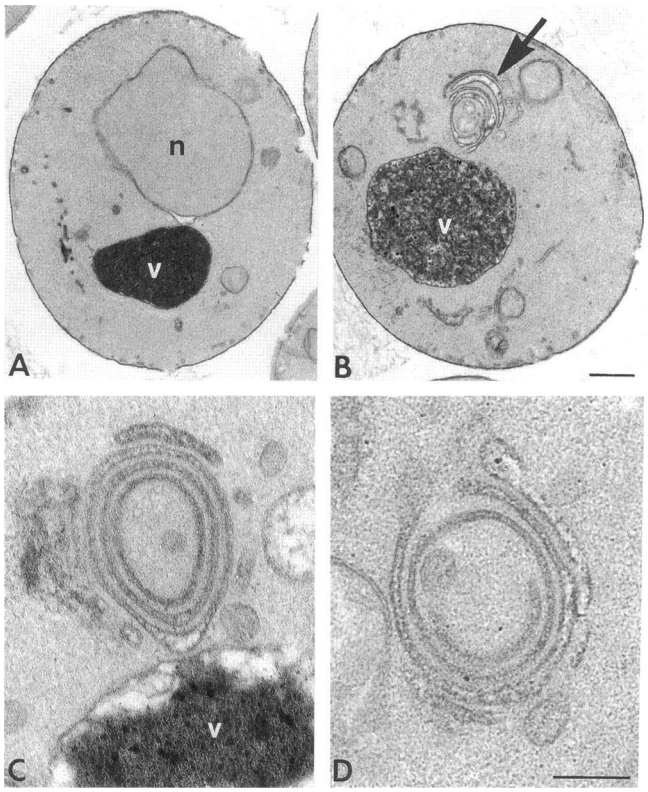

Figure 6. Electron microscopic analysis of Δ*vps28* mutant cells. (A) Wild-type (SEY6210) and (B) Δ*vps28* (KKY20) cells were fixed, embedded after treatment with osmium/thiocarbohydrazide and dehydration, and then sectioned and stained for electron microscopic analysis. The arrow indicates the stacks of curved membrane cisternae located adjacent to the vacuole in Δ*vps28* cells. Panels C and D show a higher magnification view of the cupped cisternal structures found in Δ*vps28* cells. The bar in panels A and B represents 0.5 μm. The bar in panels C and D represents 0.1 μm. (n, nucleus; v, vacuole).

The approximate size, frequency, and perivacuolar location of the aberrant structures observed either by electron or fluorescence microscopy was similar, suggesting that they may correspond to the same subcellular compartment (Figures 5–7). To determine whether this is indeed the case, the distribution of the 60-kDa V-ATPase subunit in Δ*vps28* cells was examined by immuno-electron microscopy. Ultrathin cryosections of fixed Δ*vps28* cells were incubated with a monoclonal antibody specific to the 60-kDa vacuolar ATPase subunit. This was followed by incubation with 10-nm gold anti-mouse IgG conjugate. Gold particles were found primarily on the novel cupped cisternal membranes (Figure 8, A–D). Consistent with the immunofluorescent data (Figure 5F), gold particles in

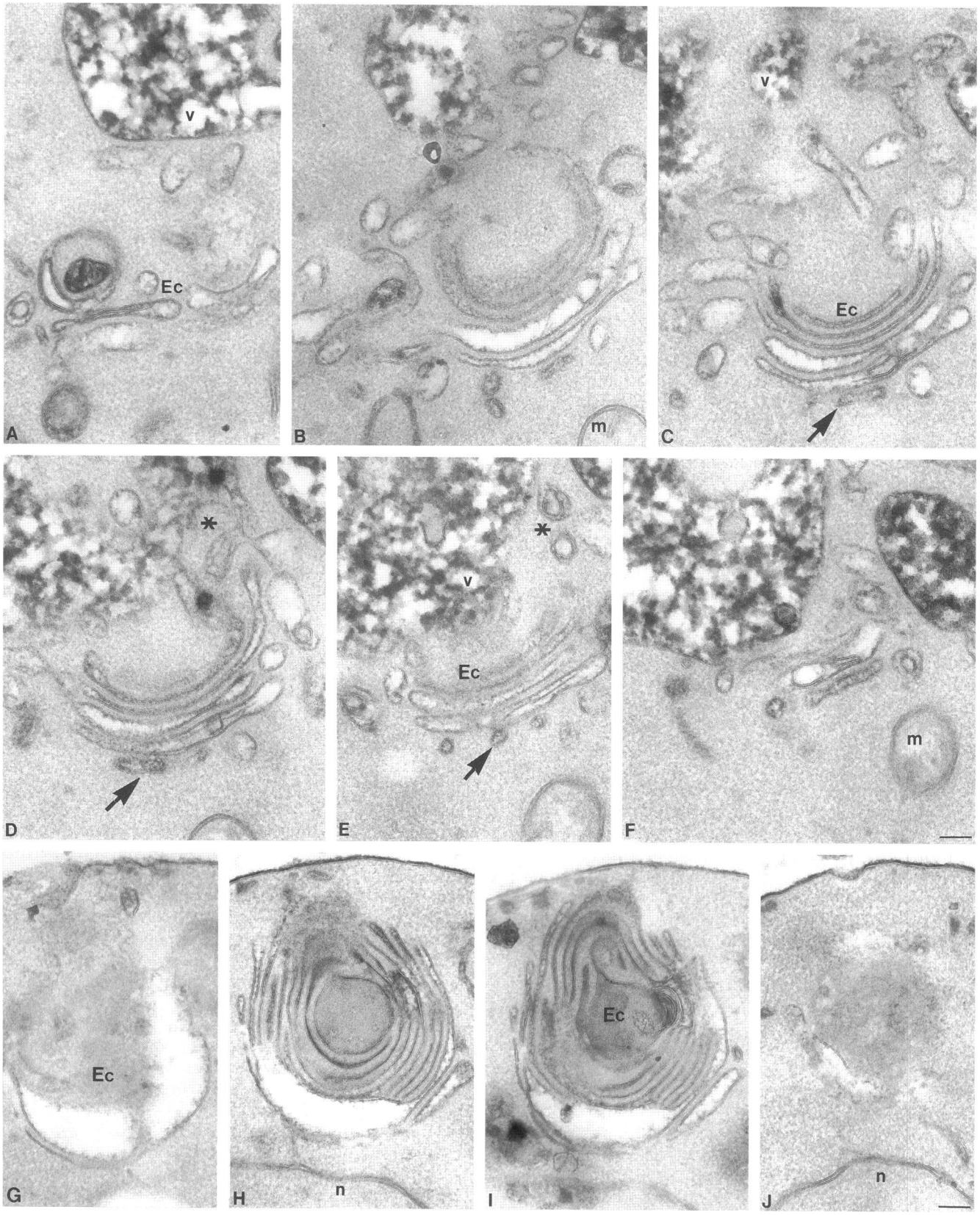

Figure 7.

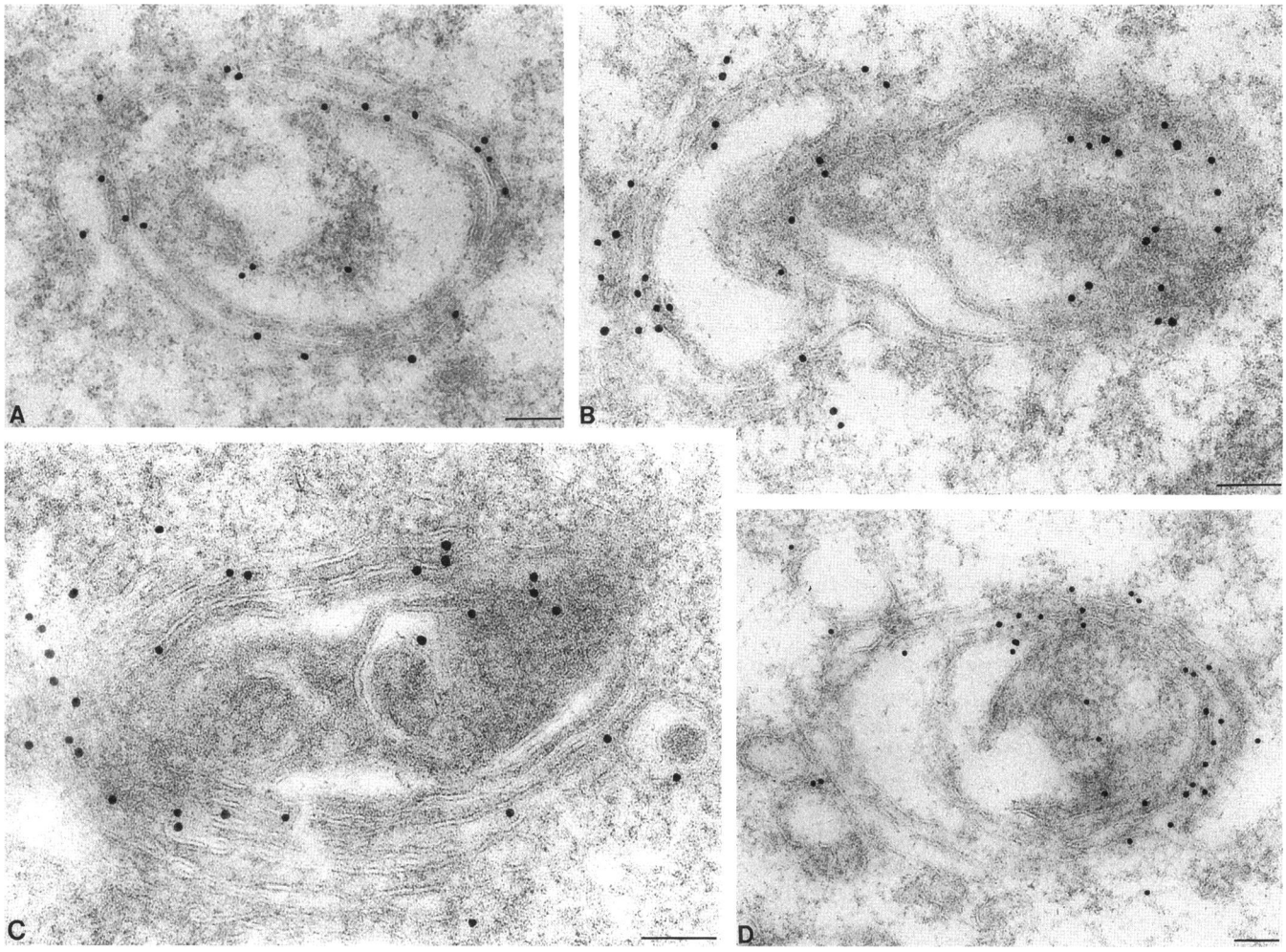

Figure 8. The vacuolar H^+-ATPase accumulates in the clusters of curved cisternal membranes found in Δ*vps28* cells. The distribution of the 60-kDa subunit of the V-ATPase in Δ*vps28* cells was determined by immuno-electron microscopy. The gold particles were primarily associated with the stacks of curved cisternal membranes, as shown in panels A–D. Consistent with the immunofluorescent data, gold particles were also associated with vacuolar membranes, as summarized in Table 2. Bars, 0.1 μm.

Δ*vps28* cells were also associated with the vacuolar membranes, as summarized in Table 2. Thus, this compartment visualized by electron microscopy is the same as the class E compartment visualized by indirect immunofluorescence for the 60-kDa V-ATPase subunit (Figure 5F). The multilamellar nature of this compartment would explain the increased fluorescent signal exhibited by the compartment when examined with the membrane dye FM 4-64 and antibodies specific for the membrane protein Ste3p and the V-ATPase (Figure 5).

DISCUSSION

VPS28 is one of the thirteen class E *VPS* genes required for efficient endocytic and biosynthetic traffic to the vacuole (Robinson *et al.*, 1988; Raymond *et al.*, 1992; Cereghino *et al.*, 1995; Piper *et al.*, 1995; Vida and

Figure 7 (cont). Serial section analysis of the novel membrane compartment found in Δ*vps28* cells. Δ*vps28* cells were fixed, processed for electron microscopy, and then serial thin-sections of about 100 nm were cut. The multilamellar class E compartment (Ec) generally consisted of either loosely cupped clusters of membrane cisternae (A–F) or of more spherical structures of tightly stacked curved cisternae (G–J). In addition, fenestrated and tubular membrane compartments were also observed (indicated by stars and arrows in C–E). (A–J) Selected sections through the class E compartment in two different Δ*vps28* cells: panels A–F were sections 1, 4, 6, 7, 8, and 10 from an 11-section set, and panels G–H were sections 2, 5, 6, and 9 from a set of nine sections through the novel membrane compartment. (n, nucleus; v, vacuole; and m, mitochondria).

Table 2. Distribution of the 60-kDa V-ATPase subunit in Δ*vps28* cells

Compartment	Density[a]
Class E compartment	41 ± 15
Vacuole	27 ± 9
Endoplasmic reticulum	<1
Plasma membrane	<1
Mitochondria	<1

[a] The density is the number of gold particles per 10 μm linear membrane.

Emr, 1995). Disruption of *VPS28* resulted in the accumulation of vacuolar and endocytic markers in an exaggerated endosome-like compartment located next to an enlarged spherical vacuole (Figures 5–8). Detailed ultrastructural analysis of this compartment revealed that it is composed of stacks of curved membrane cisternae (Figures 6–8). Unlike the majority of the *vps* mutants, the sorting defects in the class E *vps* mutants are relatively modest: 50% or less CPY is missorted (Robinson *et al.*, 1988; Raymond *et al.*, 1992). This moderate sorting defect, together with the observed presence of a vacuole containing properly localized proteins, indicates that class E *vps* mutants are not completely defective in vacuolar transport but rather exhibit a kinetic defect in both anterograde and retrograde transport out of the prevacuolar endosome. This results in the accumulation of an exaggerated multilamellar prevacuolar compartment, the class E compartment, that is likely to correspond to the site of convergence for both endocytic and biosynthetic traffic destined for the vacuole (Figures 5–8).

Vps28p Is Required for Efficient Transport out of the Prevacuolar Endosome

Disruption of *VPS28* resulted in a moderate defect (~40–50%) in processing of the soluble vacuolar protease CPY and a minor defect (~10–15%) in the maturation of the soluble vacuolar protease PrA (Figure 3). The vacuolar protein sorting defect may be due in part to inefficient retrieval of the vacuolar protein sorting receptor Vps10p as well as other late Golgi proteins from a prevacuolar endosomal compartment (Figure 5H; Cereghino *et al.*, 1995; Piper *et al.*, 1995). Mislocalization of Vps10p would result in a net decrease in receptors available in the late Golgi to mediate the delivery of vacuolar proteins to the endosome. The moderate CPY sorting defect in *vps28* cells suggests that Vps10p is able to complete several rounds of transport; thus recycling from the prevacuolar compartment to the Golgi is impaired, but not blocked, in class E *vps* mutants. The minor defect in the sorting of PrA is consistent with the observation that PrA can utilize both a Vps10p-dependent and a Vps10p-independent transport mechanism (Marcusson *et al.*, 1994; Westphal *et al.*, 1996); the latter may be less affected by the loss of Vps28p. The vacuolar membrane protein ALP was sorted and matured in Δ*vps28* cells with a minor kinetic delay (Figure 3). Indirect immunofluorescence (Raymond *et al.*, 1992) and subcellular fractionation studies (Cereghino *et al.*, 1995) indicate that ALP localizes to the vacuolar membrane of class E *vps* mutant cells; therefore, maturation of ALP in *vps28* cells is consistent with proper localization to the vacuole. As noted in earlier studies, ALP thus may utilize a different sorting mechanism than the soluble vacuolar hydrolases as reviewed in Stack *et al.* (1995).

In addition to the defect in the sorting of soluble vacuolar proteins, *vps28* mutants exhibited defects in endocytic traffic to the vacuole. The vital membrane dye FM 4-64 and the **a**-factor receptor Ste3p, which are normally transported from the plasma membrane to the vacuole via endocytosis, accumulated in the class E compartment in *vps28* cells (Figure 5). The transport of the V-ATPase was also impaired, as it was also partially located in the acidified class E compartment in *vps28* mutant cells (Figure 5). Thus Vps28p function is required for efficient transport of both membrane and protein out of the prevacuolar endosome. However, loss of Vps28p function does not completely block traffic from the endosome. Δ*vps28* cells still have a vacuole; furthermore, substantial amounts of the dye FM 4-64, the V-ATPase, and Ste3p are properly localized to the vacuole in these mutant cells (Figure 5 and Table 2).

Novel Multilamellar Structures Accumulate in Δvps28 Cells

Δ*vps28* cells contain unique stacks of curved membrane cisternae that correspond to the class E compartment (Figures 6–8). These cisternae may reflect a dramatic increase in the membrane and protein content of the prevacuolar endosome due to a kinetic imbalance in the rate of membrane flow out of the compartment relative to membrane entry into the compartment. Thus the stacks of curved cisternae observed in Δ*vps28* cells represent an exaggerated prevacuolar compartment that is unlikely to reflect normal endosomal morphology in yeast. The loss of the peroxisomal integral membrane protein Pas7p in *Pichia pastoris* leads to the accumulation of curved membrane sheets and tubules instead of normal peroxisomes (Kalish *et al.*, 1995). Also, moderate overproduction of the ER protein HMG-CoA reductase results in the accumulation of multilamellar karmellae in yeast and crystalloid ER in mammalian cells (Wright *et al.*, 1988, 1990). Thus the membrane proliferation observed in class E *vps* mutants may be due in part to aberrant accumulation of one or more membrane proteins within the prevacu-

olar compartment. The interaction between accumulated membrane receptors (i.e., SNAREs) may contribute to the closely stacked nature of the curved cisternae seen in Δ*vps28* mutant cells, as has been proposed for Golgi stacks (Warren, 1993).

The cupped stacks of membrane cisternae observed in Δ*vps28* cells look similar to organelles observed in mammalian cells, including the following: 1) the multilamellar endosomal compartment induced by the expression of major histocompatibility complex class II molecules (Amigorena *et al.*, 1994; Calafat *et al.*, 1994; Tulp *et al.*, 1994), and 2) Golgi stacks (Farquhar, 1985). Although the class E compartment has a Golgi-like morphology, this compartment does not appear to result from a fusion of the late Golgi with the endosome. The fact that protein sorting to the vacuole is only partially defective and that secretion to the cell surface is not significantly impaired in class E *vps* mutants indicates that the late Golgi is functional (Figure 3) even though some of the late Golgi proteins have been mislocalized to the class E compartment (Raymond *et al.*, 1992; Cereghino *et al.*, 1995; Piper *et al.*, 1995). Also, the α1,3-mannosyltransferase Mnn1p (Graham *et al.*, 1994) appears to maintain its normal Golgi distribution in class E *vps* mutants (Cereghino *et al.*, 1995). Furthermore, the class E compartment appears to be unable to generate vesicular traffic destined for the cell surface, since both the mature PrA and CPY that appear to partially reside in the class E compartment (Raymond *et al.*, 1992; Cereghino *et al.*, 1995) are not secreted from *vps28* mutant cells (Figure 3). Taken together, these data indicate that the class E compartment, despite its Golgi-like appearance, is an exaggerated post-Golgi prevacuolar compartment.

Class E Vps Proteins may Maintain Endosome Function and Morphology

The data presented here are consistent with a model in which Vps28p function is required for efficient transport from the endosome to both the vacuole and the late Golgi. In the absence of efficient transport out of the endosome, membrane and protein could accumulate and generate the exaggerated cupped stacks of cisternal membranes observed in Δ*vps28* mutants (Figures 5–8). Vps28p resides in the cytoplasm (Figure 4) but may associate with a membrane compartment, such as the endosome, in a weak or transient manner. Vps27p, a class E Vps protein that also resides in the cytoplasm, appears to associate with the class E compartment in class E *vps23* mutant cells (Piper *et al.*, 1995). The phenotypic similarities among the 13 different class E *vps* mutants suggest that the class E Vps proteins may function together, possibly as part of a protein complex, in the execution of a common process. Consistent with this hypothesis, over 20 class E *vps* double mutants have been constructed, and each exhibited phenotypes similar to the single class E *vps* mutant strains.

It is currently not understood how Vps28p and the other class E Vps proteins may regulate endosome function and morphology. One possibility is that Vps28p and other class E Vps proteins function as coat components that mediate the formation of endosome-to-vacuole transport intermediates, such as vesicles or tubules, emerging from the endosome. Alternatively, the class E *VPS* gene products may function to maintain a dynamic endosomal structure required for optimal transport out of the organelle, possibly by interaction with cytoskeletal elements. In mammalian cells, sorting and recycling endosomes are dynamic structures that mediate transport via tubulo-vesicular and cisternal elements (reviewed in Gruenberg and Maxfield, 1995). The class E Vps proteins may be involved in the sorting of proteins into distinct regions of the compartment, or may mediate the formation of active tubular membrane networks that dramatically enhance the rate of anterograde and retrograde transport out of the prevacuolar endosome. Isolation of a conditional allele of *vps28*, coupled with further biochemical and immunochemical characterization of the accumulated membranous structures, should provide further insight into the role of Vps28p in the maintenance of normal endosome structure and function.

ACKNOWLEDGMENTS

We are very grateful to the Electron Microscopy Core B headed by Marilyn Farquhar for outstanding assistance with the electron microscopy work (supported by Program Project grant CA58689) and to Tammie McQuistan for her excellent photographic assistance. We thank Raffi Aroian for the YCp50 library DNA and Gerhard Paravicini for construction of plasmid pGP28–1. We are grateful to Mark Rose and Bill Wickner for gifts of antisera against Kar2p and Kex2p, respectively, and to George Sprague for generously providing plasmid pSL2099 (encoding c-myc–tagged Ste3p). This work was supported by grants GM-32703 and CA-58689 (to S.D. Emr). Partial support was also provided by General Electric (to L.M. Banta). K. Köhrer was supported by a fellowship from the Deutsche Forschungsgemeinschaft. S.D. Emr is supported as an Investigator of the Howard Hughes Medical Institute. We thank members of the Emr lab, especially Beverly Wendland, for helpful comments and discussion during the preparation of this manuscript. The GenBank/EMBL accession number for the sequence reported in this paper is U50630.

REFERENCES

Amigorena, S., Drake, J.R., Webster, P., and Mellman, I. (1994). Transient accumulation of new class II MHC molecules in a novel endocytic compartment in B lymphocytes. Nature *369*, 113–120.

Anraku, Y., Umemoto, N., Hirata, R., and Ohya, Y. (1992). Genetic and cell biological aspects of the yeast vacuolar H^+-ATPase. J. Bioenerg. Biomembr. *24*, 395–405.

Ausubel, F.M., Brent, R., Kingston, R.E., Moore, D.D., Seidman, J.G., Smith, J.A., and Struhl, K. (1987). Current Protocols in Molecular Biology Pages, New York: John Wiley and Sons.

Bankaitis, V.A., Johnson, L.M., and Emr, S.D. (1986). Isolation of yeast mutants defective in protein targeting to the vacuole. Proc. Natl. Acad. Sci. USA *83*, 9075–9079.

Banta, L.M., Robinson, J.S., Klionsky, D.J., and Emr, S.D. (1988). Organelle assembly in yeast: characterization of yeast mutants defective in vacuolar biogenesis and protein sorting. J. Cell Biol. *107*, 1369–1383.

Bullock, W.O., Ferandez, J.M., and Short, J.M. (1987). Biotechniques *5*, 376–379.

Calafat, J., Nijenhuis, M., Janssen, H., Tulp, A., Dusseljee, S., Wubbolts, R., and Neefjes, J. (1994). Major histocompatibility complex class II molecules induce the formation of endocytic MIIC-like structures. J. Cell Biol. *126*, 967–977.

Casadaban, M.J., and Cohen, S.N. (1980). Analysis of gene control signals by DNA fusion and cloning in *Escherichia coli*. J. Mol. Biol. *138*, 179–207.

Cereghino, J.L., Marcusson, E.G., and Emr, S.D. (1995). The cytoplasmic tail domain of the vacuolar sorting receptor Vps10p and a subset of *VPS* gene products regulate receptor stability, function, and localization. Mol. Biol. Cell *6*, 1089–1102.

Davis, N.G., Horecka, J.L., and Sprague, G.F. (1993). *Cis*-acting and *trans*-acting functions required for endocytosis of the yeast pheromone receptors. J. Cell Biol. *122*, 53–65.

Dieckmann, C.L., and Tzagoloff, A. (1985). Assembly of the mitochondrial membrane system. J. Biol. Chem. *260*, 1513–1520.

Farquhar, M.G. (1985). Progression in unraveling pathways of Golgi traffic. Annu. Rev. Cell Biol. *1*, 447–488.

Feinberg, A.P., and Vogelstein, B. (1984). A technique for radiolabeling DNA restriction endonuclease fragments to high specific activity. Anal. Biochem. *137*, 266–267.

Graham, T.R., and Emr, S.D. (1991). Compartmental organization of Golgi-specific protein modification and vacuolar protein sorting events defined in a yeast *sec18* (NSF) mutant. J. Cell Biol. *114*, 207–218.

Graham, T.R., Seeger, M., Payne, G.S., MacKay, V.L., and Emr, S.D. (1994). Clathrin-dependent localization of α1,3 mannosyltransferase to the Golgi complex of *Saccharomyces cerevisiae*. J. Cell Biol. *127*, 667–678.

Gruenberg, J., and Maxfield, F.R. (1995). Membrane transport in the endocytic pathway. Curr. Opinion Cell Biol. *4*, 552–563.

Herman, P.K., and Emr, S.D. (1990). Characterization of *VPS34*, a gene required for vacuolar protein sorting and vacuole segregation in *Saccharomyces cerevisiae*. Mol. Cell. Biol. *10*, 6742–6754.

Herman, P.K., Stack, J.H., and Emr, S.D. (1991). A genetic and structural analysis of the yeast Vps15 protein kinase: evidence for a direct role of Vps15p in vacuolar protein delivery. EMBO J. *13*, 4049–4060.

Horazdovsky, B.F., Busch, G.R., and Emr, S.D. (1994). *VPS21* encodes a rab5-like GTP binding protein that is required for the sorting of yeast vacuolar proteins. EMBO J. *13*, 1297–1309.

Ito, H., Fukada, Y., Murata, K., and Kimura, A. (1983). Transformation of intact yeast cells treated with alkali cations. J. Bacteriol. *153*, 163–168.

Johnson, L.M., Bankaitis, V.A., and Emr, S.D. (1987). Distinct sequence determinants direct intracellular sorting and modification of a yeast vacuolar protease. Cell *48*, 875–885.

Jones, E.W. (1977). Proteinase mutants of *Saccharomyces cerevisiae*. Genetics *85*, 23–33.

Jones, E.W. (1984). The synthesis and function of proteases in *Saccharomyces*: genetic approaches. Annu. Rev. Genet. *18*, 233–270.

Kalish, J.E., Theda, C., Morrell, J.C., Berg, J.M., and Gould, S.J. (1995). Formation of the peroxisome lumen is abolished by loss of *Pichia pastoris* Pas7p, a zinc-binding integral membrane protein of the peroxisome. Mol. Cell. Biol. *15*, 6406–6419.

Kane, P.M., Kuehn, M.C., Howald-Stevenson, I., and Stevens, T.H. (1992). Assembly and targeting of peripheral and integral membrane subunits of the yeast vacuolar H(+)-ATPase. J. Biol. Chem. *267*, 447–454.

Kane, P.M., and Stevens, T.H. (1992). Subunit composition, biosynthesis, and assembly of the yeast vacuolar proton-translocation ATPase. J. Bioenerg. Biomembr. *24*, 383–393.

Klionsky, D.J., Banta, L.M., and Emr, S.D. (1988). Intracellular sorting and processing of a yeast vacuolar hydrolase: proteinase A propeptide contains vacuolar targeting information. Mol. Cell. Biol. *8*, 2105–2116.

Klionsky, D.J., and Emr, S.D. (1989). Membrane protein sorting: biosynthesis, transport and processing of yeast vacuolar alkaline phosphatase. EMBO J. *8*, 2241–2250.

Köhrer, K., and Domdey, H. (1991). Preparation of high molecular weight RNA. Methods Enzymol. *194*, 398–405.

Köhrer, K., and Emr, S.D. (1993). The yeast *VPS17* gene encodes a membrane-associated protein required for the sorting of soluble vacuolar hydrolases. J. Biol. Chem. *268*, 559–569.

Kornfeld, S. (1992). Structure and function of the mannose 6-phosphate/insulin-like growth factor II receptors. Annu. Rev. Biochem. *61*, 307–330.

Kyte, J., and Doolittle, R. (1982). A simple method for displaying the hydropathic character of a protein. J. Mol. Biol. *157*, 105–132.

Maniatis, T., Fritsch, E.F., and Sambrook, J. (1982). Molecular Cloning: A Laboratory Manual, Cold Spring Harbor, NY: Cold Spring Harbor Laboratory Press.

Marcusson, E.G., Horazdovsky, B.F., Cereghino, J.L., Gharakhanian, E., and Emr, S.D. (1994). The sorting receptor for yeast vacuolar carboxypeptidase Y is encoded by the *VPS10* gene. Cell *77*, 579–586.

Miller, J. (1972). Experiments in Molecular Genetics Pages, Cold Spring Harbor, NY: Cold Spring Harbor Laboratory Press.

Nelson, N. (1992). Structural conservation and functional diversity of V-ATPases. J. Bioenerg. Biomembr. *24*, 407–414.

Orr-Weaver, T.L., Szostak, J.W., and Rothstein, R.J. (1983). Genetic application of yeast transformation with linear and gapped plasmids. Methods Enzymol. *101*, 228–245.

Paravicini, G., Horazdovsky, B.F., and Emr, S.D. (1992). Alternative pathways for the sorting of soluble vacuolar proteins in yeast: a *vps35* null mutant missorts and secretes only a subset of vacuolar hydrolases. Mol. Biol. Cell *3*, 415–427.

Piper, R.C., Cooper, A.A., Yang, H., and Stevens, T.H. (1995). *VPS27* controls vacuolar and endocytic traffic through a prevacuolar compartment in *Saccharomyces cerevisiae*. J. Cell Biol. *131*, 603–617.

Raymond, C.K., Howald-Stevenson, I., Vater, C.A., and Stevens, T.H. (1992). Morphological classification of the yeast vacuolar protein sorting mutants: evidence for a prevacuolar compartment in class E *vps* mutants. Mol. Biol. Cell *3*, 1389–1402.

Raymond, C.K., Roberts, C.J., Moore, K.E., Howald, I., and Stevens, T.H. (1992). Biogenesis of the vacuole in *Saccharomyces cerevisiae*. Int. Rev. Cytol. *139*, 59–120.

Redding, K., Holcomb, C., and Fuller, R.S. (1991). Immunolocalization of Kex2 protease identifies a putative late Golgi compartment in the yeast *Saccharomyces cerevisiae*. J. Cell Biol. *113*, 527–538.

Robinson, J.S., Klionsky, D.J., Banta, L.M., and Emr, S.D. (1988). Protein sorting in *Saccharomyces cerevisiae*: isolation of mutants de-

fective in the delivery and processing of multiple vacuolar hydrolases. Mol. Cell. Biol. *8*, 4936–4948.

Rose, M., Novick, P., Thomas, J., Botstein, D., and Fink, G. (1987). A *Saccharomyces cerevisiae* genomic plasmid bank based on centromere containing shuttle vector. Gene *60*, 237–244.

Rothman, J.H., and Stevens, T.H. (1986). Protein sorting in yeast: mutants defective in vacuole biogenesis mislocalize vacuolar proteins into the late secretory pathway. Cell *47*, 1041–1051.

Rothstein, R.J. (1983). One-step gene disruption in yeast. Methods Enzymol. *101*, 202–212.

Sanger, F., Nicklen, F., and Coulson, A.R. (1977). DNA sequencing with chain-terminating inhibitors. Proc. Natl. Acad. Sci. USA *74*, 5463–5467.

Schimmöller, F., and Riezman, H. (1993). Involvement of Ypt7p, a small GTPase, in traffic from late endosome to the vacuole in yeast. J. Cell Sci. *106*, 823–830.

Sherman, F. (1991). Getting started with yeast. Methods Enzymol. *194*, 3–21.

Sherman, F., Fink, G.R., and Lawrence, L.W. (1979). Methods in Yeast Genetics: A Laboratory Manual, Cold Spring Harbor, NY: Cold Spring Harbor Laboratory Press.

Sikorski, R.S., and Hieter, P. (1989). A system of shuttle vectors and yeast host strains designed for efficient manipulation of DNA in *Saccharomyces cerevisiae*. Genetics *122*, 19–27.

Singer, B., and Riezman, H. (1990). Detection of an intermediate compartment involved in transport of alpha-factor from the plasma membrane to the vacuole in yeast. J. Cell Biol. *110*, 1911–1922.

Southern, E.M. (1975). Detection of specific sequences among DNA fragments separated by gel electrophoresis. J. Mol. Biol. *89*, 503–517.

Stack, J.H., Horazdovsky, B.F., and Emr, S.D. (1995). Receptor-mediated protein sorting to the vacuole in yeast: roles for a protein kinase, a lipid kinase and GTP-binding proteins. Annu. Rev. Cell Dev. Biol. *11*, 1–33.

Stevens, T., Esmon, B., and Schekman, R. (1982). Early stages in the yeast secretory pathway are required for transport of carboxypeptidase Y to the vacuole. Cell *30*, 439–448.

Struhl, K. (1987). Promoters, activator proteins, and the mechanism of transcriptional initiation in yeast. Cell *49*, 295–297.

Tulp, A., Verwoerd, D., Dobberstein, B., Ploegh, H.L., and Pieters, J. (1994). Isolation and characterization of the intracellular MHC class II compartment. Nature *369*, 120–126.

Valls, L.A., Hunter, C.P., Rothman, J.H., and Stevens, T.H. (1987). Protein sorting in yeast: the localization determinant of yeast vacuolar carboxypeptidase Y resides in the propeptide. Cell *48*, 887–897.

Valls, L.A., Winther, J.R., and Stevens, T.H. (1990). Yeast carboxypeptidase Y vacuolar targeting signal is defined by four propeptide amino acids. J. Cell Biol. *111*, 361–368.

Vida, T.A., and Emr, S.D. (1995). A new vital stain for visualizing vacuolar membrane dynamics and endocytosis in yeast. J. Cell Biol. *128*, 779–792.

Vida, T.A., Huyer, G., and Emr, S.D. (1993). Yeast vacuolar proenzymes are sorted in the late Golgi complex and transported to the vacuole via a prevacuolar endosome-like compartment. J. Cell Biol. *121*, 1245–1256.

Warren, G. (1993). Cell biology: bridging the gap. Nature *362*, 297–298.

Westphal, V., Marcusson, E., Winther, J.R., Emr, S.D., and van den Hazel, B. (1996). Multiple pathways for vacuolar sorting of yeast proteinase A. J. Biol. Chem. (*in press*).

Wickerham, L.J. (1946). A critical evaluation of the nitrogen assimilation tests commonly used in the classification of yeasts. J. Bacteriol. *52*, 293–301.

Wilimzig, M. (1985). LiCl-boiling method for plasmid mini-preps. Trends Genet. *1*, 158.

Wright, R., Basson, M., D'Ari, L., and Rine, J. (1988). Increased amounts of HMG-CoA reductase induce "karmellae": a proliferation of stacked membrane pairs surrounding the yeast nucleus. J. Cell Biol. *107*, 101–114.

Wright, R., Keller, G., Gould, S.J., Subramani, S., and Rine, J. (1990). Cell-type control of membrane biogenesis induced by HMG-CoA reductase. New Biol. *2*, 915–921.

Yanisch-Perron, C., Vieira, J., and Messing, J. (1985). Improved M13 phage cloning vectors and host strains: nucleotide sequences of the M13mp18 and pUC19 vectors. Gene *33*, 103–109.

Zaret, K.S., and Sherman, F. (1982). DNA sequence required for efficient transcription termination in yeast. Cell *28*, 563–573.